Proc. Natl. Acad. Sci. USA
Vol. 89, pp. 4801–4805, June 1992
Biophysics

Mass determination and estimation of subunit stoichiometry of the bacterial hook–basal body flagellar complex of *Salmonella typhimurium* by scanning transmission electron microscopy

(bacterial chemotaxis/mass measurement/cryoelectron microscopy/bacterial motility/molecular motors)

GINA E. SOSINSKY*†, NOREEN R. FRANCIS*, DAVID J. DEROSIER*, JOSEPH S. WALL‡, MARTHA N. SIMON‡, AND JAMES HAINFELD‡

*Rosenstiel Basic Medical Sciences Research Center, Brandeis University, Waltham, MA 02254-9110; and ‡Department of Biology, Brookhaven National Laboratory, Upton, NY 11973

Communicated by Hugh E. Huxley, February 24, 1992 (received for review December 2, 1991)

ABSTRACT **The basal body, a part of the rotary motor of the bacterial flagellum, is a multiprotein assembly that consists of four rings (denoted M, S, P, and L) and an axial rod (denoted R). From analysis of scanning transmission electron microscopy images of hook–basal body preparations isolated from *Salmonella typhimurium*, we have determined the masses of the basal body and three of its subcomplexes. The mass of the basal body (i.e., the four rings and rod) is 4400 ± 490 kDa (mean ± SD; n = 54). The mass of the LPR subcomplex (i.e., L and P rings and the whole rod) is 2600 ± 380 kDa (n = 55), that of the L and P rings and the distal part of the rod is 2100 ± 320 kDa (n = 25), and the mass of the L and P ring subcomplex is 1700 ± 260 kDa (n = 514). These results, together with the masses of the component proteins, indicate that the rings contain ≈26 subunits each and that the mass of the rod is consistent with a composition of ≈6 copies each of three of the rod proteins FlgB, FlgC, and FlgF and ≈26 copies of FlgG as determined by Jones *et al.* [Jones, C. J., Macnab, R. M., Okino, H. & Aizawa, S.-I. (1990) *J. Mol. Biol.* 212, 377–387] using quantitative gel electrophoresis. The results of Jones *et al.*, together with ours, account for all proteins in the basal body to within ≈5% (or 200 kDa).**

The bacterial flagellum, the organelle responsible for cell motility, is a macromolecular assembly consisting of multiple copies of at least 13 different proteins. The flagellum contains an axial structure running its entire length and a set of ring structures that are localized in the basal body (see Fig. 1 *Inset*). In *Salmonella typhimurium*, the components of the axial structure, in cell proximal-to-distal order, are FlgB, FlgC, and FlgF (proximal rod proteins); FlgG (distal rod protein); FlgE (hook protein); FlgK and FlgL (HAP1 and HAP3, the filament–hook junction proteins); FliC (flagellin, the filament protein); and FliD (HAP2, the filament capping protein). The basal body, the part of the flagellum embedded in the cell envelope, contains four rings—M, S, L, and P. The M ring is made from the FliF protein (1), which also makes up the S ring and the cell proximal part of the rod (T. Ueno, K. Oosawa, and S.-I. Aizawa, personal communication). The P ring and the L ring are composed of FlgH and FlgI, respectively (2). An additional protein, FliE, is also a basal body protein, but its location is unknown (3).

In an earlier paper, we described the hook–basal body complex (HBB) and its subcomplexes obtained by dissociation in acid (4). Using low-dose electron cryomicroscopy and image-averaging techniques, we computed averages of the HBB and four subcomplexes at ≈25 Å resolution. In these averaged images, the S, P, and L rings appear cylindrically symmetric, but the M ring shows some evidence of angular periodicity. We were unable to deduce the subunit symmetry of the constituent proteins from these reconstructions or from the individual images of isolated L–P ring structures (LP) lying *en face*.

Jones *et al.* (5) determined the stoichiometries of HBB by quantitative gel autoradiography. They determined that the number of FliF subunits in the M ring was ≈26. The L and P rings also contained ≈26 copies of their subunit proteins. [See Table 1 for a summary of the data of Jones *et al.* (5).] These values are in contrast with reported estimates of ring rotational symmetries of 16 (6) or 12 (7), which were based on inspection of electron microscope images of negatively stained isolated LP. In addition, freeze-fracture electron micrographs of *Escherichia coli* cell membranes contain rings of 11 or 12 intramembranous particles, which are thought to be the MotA and MotB proteins (8). However, it is not known whether these rings interact with the M ring or should be of equivalent rotational symmetry.

To obtain estimates of the number of proteins in these subassemblies, we have carried out a scanning transmission electron microscopic (STEM) analysis of the flagellar HBB. The number of elastically scattered electrons in a STEM image is proportional to the mass of the particle and, when calibrated against a standard sample, gives absolute mass values (9, 10). In the HBB, the number of subunits can be calculated because the molecular masses of the basal body proteins have been obtained from gene sequence analysis (11–13). In this paper, we present STEM images of the HBB and subcomplexes, their measured masses, and the calculated subunit stoichiometry.

Our method is entirely different from that of Jones *et al.* (5) and is subject to different errors. Jones *et al.* measured relative stoichiometries of each of the components detected on electrophoresis gels. Then, assuming that the hook contained 126 subunits (a possible source of systematic error), they determined absolute stoichiometries. In an estimate of the total mass of the basal body, the errors from the separate estimates of stoichiometry are cumulative. In our work, we directly measured the masses of the complex and subcomplexes, which requires no assumptions about protein composition. The results of these two techniques provide independent checks of each other and, taken together, show that

The publication costs of this article were defrayed in part by page charge payment. This article must therefore be hereby marked "*advertisement*" in accordance with 18 U.S.C. §1734 solely to indicate this fact.

Abbreviations: HBB, hook–basal body complex; HLPRS, complexes containing hook, L, P, and S rings, and whole rod (minus M ring); HLPR, complexes containing hook, L and P rings, and whole rod (minus M and S rings); HLP, complexes containing hook, L and P rings, and distal portion of rod (minus M and S rings and proximal rod); LP, L–P ring complex; STEM, scanning transmission electron microscopy; TMV, tobacco mosaic virus.

†To whom reprint requests should be addressed.

the stoichiometry obtained by Jones *et al.* (5) correctly accounts for the mass of the basal body to within ≈200 kDa.

MATERIALS AND METHODS

Purification of HBBs and Subcomplexes. HBBs and subcomplexes were prepared from *Salmonella* ST1 as described (4). Briefly, HBBs were isolated by the method of Aizawa *et al.* (14). Subcomplexes were produced by incubation of HBBs in 50 mM glycine/0.1% Triton X-100 buffer at pH 4, pH 3, pH 2.5, or pH 2 for various time intervals.

Preparation of Specimens for Electron Microscopy. Negatively stained and frozen-hydrated specimens were prepared and recorded under the conditions described (4).

STEM images were recorded at Brookhaven National Laboratory by the method of Wall and Hainfeld (9). A 3- to 5-μl sample of tobacco mosaic virus (TMV) (0.1 mg/ml), to be used as an internal mass standard (15), was placed on a thin (≈20 Å) hydrophilic carbon film (16) supported on a titanium grid. A 3- to 5-μl droplet of a preparation of HBB or its subcomplexes was applied next. After 1 min, the grid was blotted and washed with ≈10 drops of distilled water. The grid was quick-frozen and freeze-dried over several hours (usually overnight). STEM images were recorded at ≈4 $e^-/Å^2$ at a specimen temperature of −130°C.

Digital Image Processing. The factor that converts STEM scattering intensity to mass is usually obtained by using the TMV standard included in the preparations. This was the procedure used in measuring the mass of the LP complex. The mass of the LP complex was computed from integrated scattered intensity inside a circle slightly larger than the LP complex diameter (≈350 Å). For unknown reasons, the TMV was not an adequate standard (17) in measuring the masses of hook-containing complexes. For these structures, three sets of measurements were made: (*i*) total scattering intensity of the particle I_{HC}, (*ii*) hook linear scattering intensity $I_{H/L}$, and (*iii*) hook length L_H. Each hook-containing complex was defined by an irregular box that hugged the outer edges and the intensities inside the box were added to give I_{HC}. The value for $I_{H/L}$ was obtained in the same way as was that for the TMV. The L_H for each particle was defined as the contour length from the smaller edge of an LP trapezoid to the hook tip (see Fig. 2). We used the value of $I_{H/L}$ for the hook to compute the factor that converts scattering intensity to mass. The hook protein subunit has a mass of 42 kDa (13) and a rise per subunit of 4.1 Å (18). This corresponds to a mass/length of 10.2 kDa/Å. The mass of a hook-containing complex M_{HC} is therefore

$$M_{HC} = I_{HC} \times \frac{10.2 \text{ kDa/Å}}{I_{H/L}}.$$

The mass of the hook was then subtracted from the mass of the hook-containing complex to obtain the mass of the complex alone (M_C). The relevant equation is

$$M_C = M_{HC} - 10.2\, L_H.$$

RESULTS

Particle Selection. In our earlier paper (4), we found conditions in which we could isolate heterogeneous populations of disassembled HBBs (Fig. 1). Our acid-treated preparations contained four HBB-derived structures: (*i*) HBBs missing the M ring (HLPRS), (*ii*) HBBs lacking the M and S rings

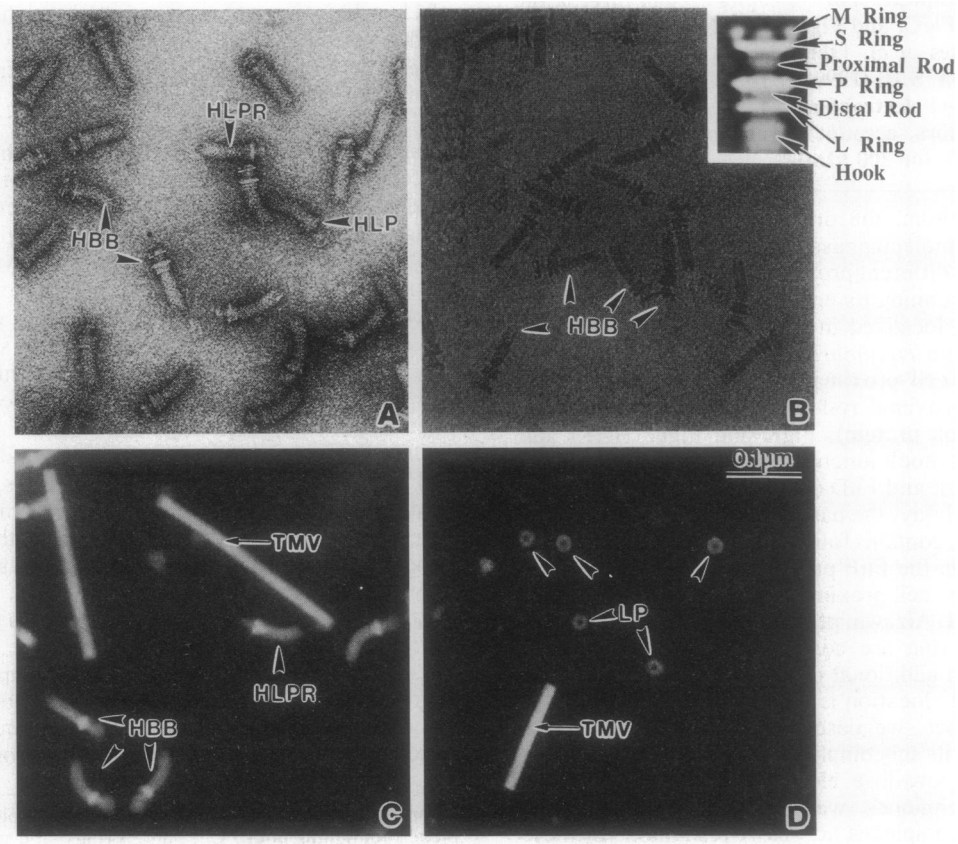

FIG. 1. Comparison between negatively stained, freeze-hydrated, and freeze-dried HBBs and subcomplexes. (*A*) Low-irradiation conventional electron microscopic image of uranyl acetate-stained HBBs and subcomplexes at pH 3. (*B*) Cryoelectron micrograph of freeze-hydrated HBBs and subcomplexes at pH 4. (*C*) STEM image of freeze-dried HBBs and subcomplexes at pH 3. (*D*) STEM image of *en face* views of freeze-dried LP ring complexes. TMV particles in *C* and *D* are used for mass calibrations. [*Inset*, reproduced from ref. 4 with permission (copyright, Academic Press).]

(HLPR), (*iii*) HBBs lacking the M and S rings and the proximal rod (HLP), and (*iv*) LP.

Our initial data set contained 1683 hook-containing subcomplexes and 514 LP rings. Among the 1683 were particles we could not classify with certainty. Five examples are shown in Fig. 2 (*Bottom*). From the set of 1683 particles, we selected only those we could unambiguously categorize. We found we could not distinguish HPLRS structures in our STEM images. Our final data set contained 54 HBBs, 55 HLPRs, and 25 HLPs. We found that the LP ring preparations were homogeneous enough to include all 514 rings in the data analysis. Fig. 2 contains five examples of each category of particle.

Mass Analysis. The histogram of masses (e.g., see Fig. 3*A1*) of the complete HBB showed considerable spread. One source of the spread was due to discrepancies in the apparent scattering constant determined from the TMV standard. The problem is evident in the variability in the measured mass/length of the hook using TMV as the standard. Ideally, the mass/length should be a constant 10.2 kDa/Å. Fig. 3*B* shows a scatter plot of HBB mass vs. mass/length of the hook portion. The average (± SD) measured mass/length of the hook was 10.9 ± 1.1 kDa/Å (n = 134). The positive correlation reinforces the idea that the TMV standard is inadequate; however, correcting for the hook mass/length usually changed the total mass by 10–15% or less. We therefore used the hook as the standard (see *Materials and Methods*). Fig. 3*A2* shows the histogram where the hook is used as the scattering standard.

Variation in the hook length causes variation in hook mass and will contribute to a real spread in the HBB masses (Fig. 3 *C* and *D*). Fig. 3*C* shows a scatter plot of hook length vs. HBB mass using TMV as the standard, and Fig. 3*D* shows the same plot using the hook as a standard. The positive correlation in both cases argues the need for a correction to the basal body mass based on hook length (see *Materials and Methods*). After subtracting the mass of the hook from that of the HBB, the scatter in mass measurements is reduced (Fig. 3*A3*).

We applied the corrections to all three sets of hook-containing complexes and calculated an average (± SD) mass from the average of the populations of each of the four complexes (Fig. 4). The average (± SD) mass of the basal body was 4400 ± 490 kDa, that of the LP and the whole rod portion of the basal body was 2600 ± 380 kDa, and that for the LP and the distal rod was 2100 ± 320 kDa. The LP mass was 1700 ± 260 kDa.

DISCUSSION

Comparison of Different Preparative Procedures. The advantage of using STEM images to measure molecular mass is that one can analyze heterogeneous samples provided the different classes of particles are discernible from each other. Since we had been able to sort the particles in our low-irradiation images for image averaging, we anticipated that we would be able to sort the particles into the same categories for molecular mass determination.

A comparison of fields of particles between the three specimen preparation techniques—negative staining, freeze-hydrating, and freeze-drying (Fig. 1)—shows that structural preservation, as judged by the clarity of the rings, is not as good in the STEM images as in the conventional electron microscopic images. This is probably due to the difference between the sample preparation techniques (vitrification vs. freeze-drying) rather than the imaging conditions.

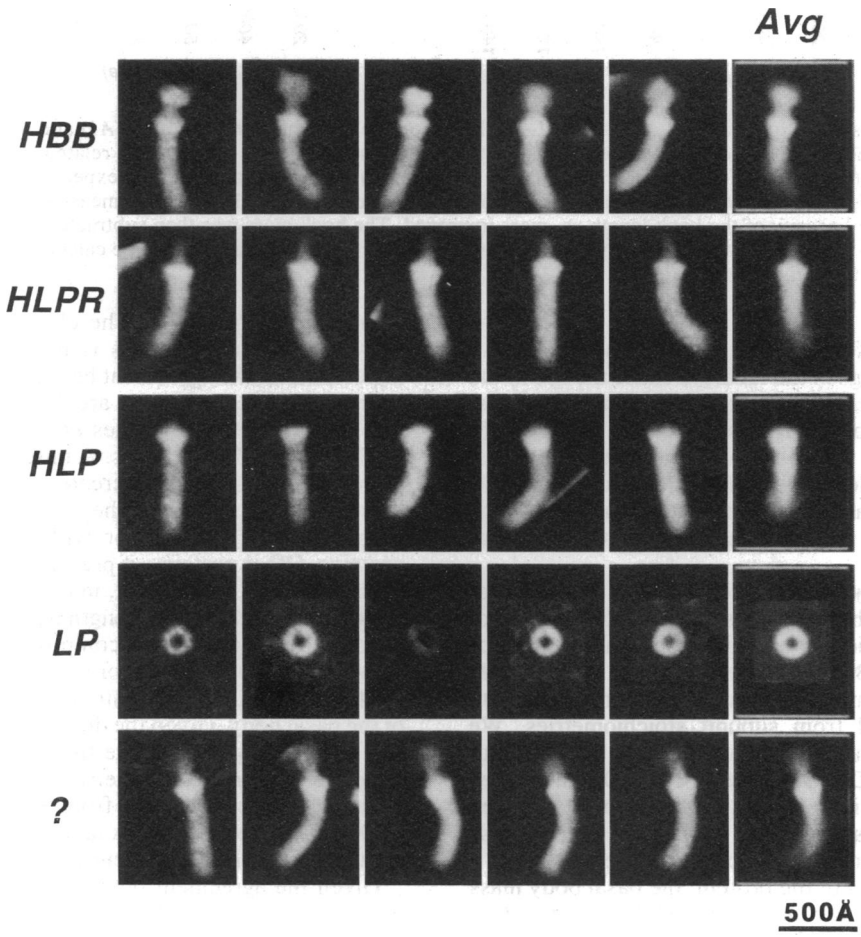

FIG. 2. Gallery of STEM images of HBBs and subcomplexes. Five representative particles from each data set and their averaged image are shown. Bottom row contains five examples of particles we could not categorize definitely as HBB, HLPRS, or HLPR.

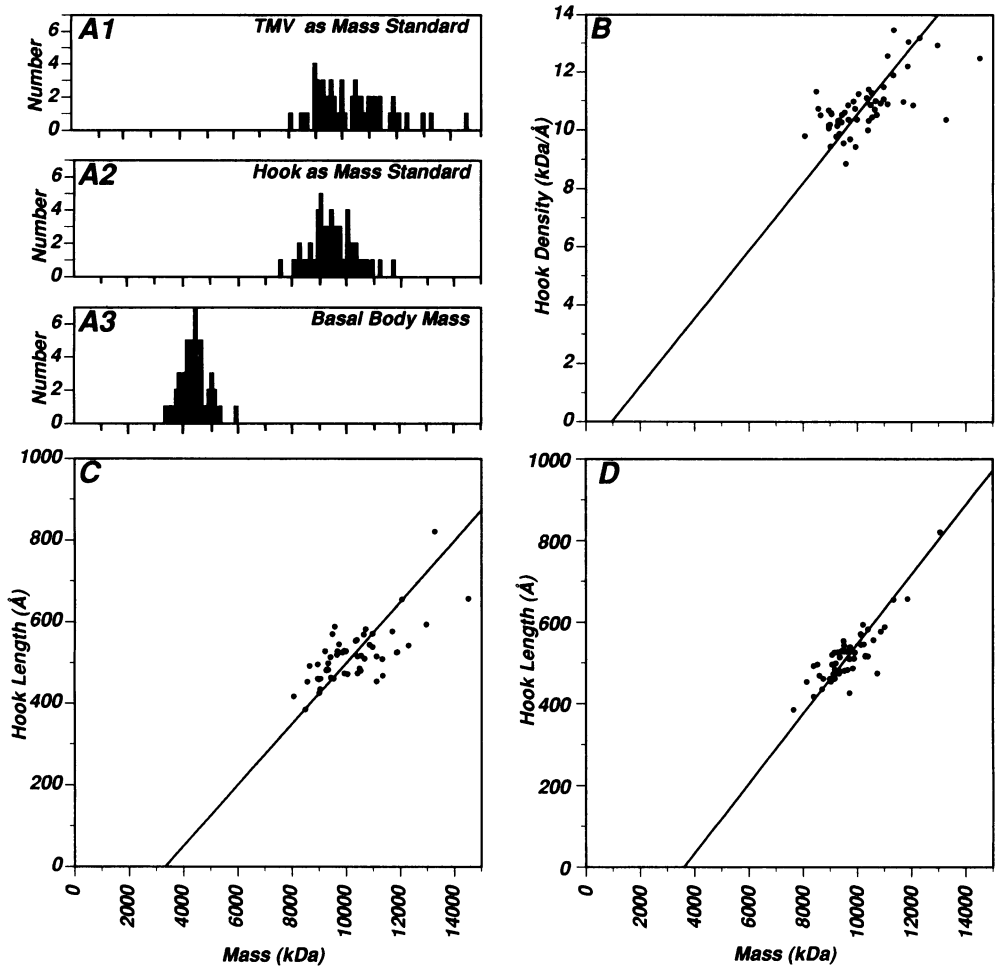

FIG. 3. Analysis of mass data for the HBB data set. (*A1–A3*) Effect on the mass histograms before (*A1*) and after (*A2*) hook mass/length correction and after subtraction of the total hook mass (*A3*). We found that the HBB mass was linearly related to hook mass/length (*B*) and hook length (*C*). From the three-dimensional reconstruction of the hook (13, 18), the hook mass/length is expected to be 10.2 kDa/Å. The hook mass/length measurements ranged from 8 to 13 kDa/Å. (*D*) After a correction factor of 10.2 kDa/Å measured hook mass/length was applied to the total hook, the linearity of the hook length vs. mass improved. The hook mass was then subtracted from the total mass to obtain the basal body mass. After these corrections were applied, the average (± SD) of the basal body could be calculated from the mass histogram. The mass scale (*x* axis) is the same for all graphs.

The combined effect of rinsing the grids with water to remove excess Triton X-100 and of freeze-drying seemed to collapse the M and S rings in the HBB, to cause the rod in the HLPR to splay, and to cause partial dissociation of the rings. Therefore, we only chose particles we could classify with certainty based on our previous structural studies (4). Discarding the questionable particles (such as those in Fig. 2 *Bottom*) reduced the scatter in the measured masses and was important in obtaining accurate mass measurements from STEM data.

Subunit Stoichiometry. Table 1 contains a summary of molecular masses, number of copies, and substructure associated with each specific protein based on quantification of SDS/PAGE of the HBB proteins from Jones *et al.* (5). Table 2 is a comparison of the masses we calculated from STEM data with masses calculated from subunit stoichiometries. We calculated the expected mass of the whole basal body without the hook to be ≈4300 kDa. Our results (4400 kDa) thus agree with Jones *et al.* (5) to within 5%. The larger errors associated with the calculated masses of Jones *et al.* are in part because the errors from each component are cumulative (19).

In addition to the mass of the protein, the basal body mass in STEM measurement may include bound detergent and/or bound lipid, which may not be adequately accounted for in the TMV or the hook standard. Both the L and M rings may have bound detergent and lipid because both are integral membrane proteins (11). The close agreement between the two methods suggests this is not a serious problem. The importance of the agreement between the two measurements is that the sources of errors are different in the two methods. The stoichiometries of Jones *et al.* (5) assumed an average hook length of 126 subunits. A miscalculation in the number of hook subunits would create a systematic error in the estimate of all proteins. They assumed also that the basal body contained just seven or, with the inclusion of FliE, eight proteins. Other proteins, if present, would not be included in the calculation. In contrast, in our work we assume that the hook is of constant mass/length but of varying length and we make no assumption about composition of the basal body. An error in hook mass/length or systematic mismeasurement of the hook length would create a systematic error in the mass of the basal body. Given the differences in the two techniques and errors, it is remarkable that all four masses calculated from the protein stoichiometric analysis and the four corresponding masses measured from STEM images are all within ≈200 kDa. The two results taken together account for both the total mass and the protein composition of the basal body.

Given the agreement between the two kinds of measurements, there can be little doubt that the M/S, L, and P ring subunits contain ≈26 proteins each. Although some images of the LP complexes obtained from highly irradiated, negatively stained specimens hint at the LP complexes containing

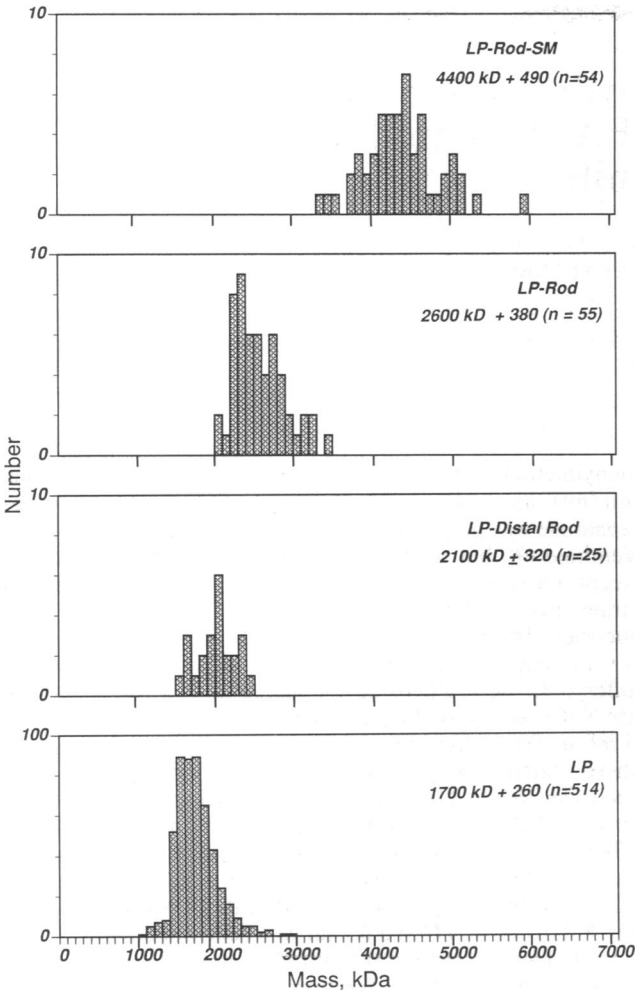

FIG. 4. Histograms of the mass populations of HBBs and subcomplexes. Histograms of the HBB, HLPR, HLP, and LP data sets were computed. The average mass ± SD and number of particles are shown for each data set.

twelvefold annular periodicity (7) or sixteenfold symmetry (6), we did not detect any twelve- or sixteenfold symmetry in our low-irradiation negatively stained or freeze-hydrated images. Inspection of images of negatively stained two-dimensional lipid reconstituted arrays of the LP ring complex (20) also failed to reveal any consistent detectable symmetry, although Akiba *et al.* (20) estimated the rotational symmetry to be ≈20. Indeed, in order to resolve 26 subunits in a 260-Å-diameter ring, one would need at least 25 Å resolution.

The numerology of the flagellum is still a puzzle. The value of 26 subunits per ring has yet to be reconciled with the 8 torque-generating units found by Blair and Berg (21) or the 11

Table 1. Summary of the known basal body proteins, their molecular mass calculated from gene sequencing, stoichiometry, and morphological location

Protein	Molecular mass, kDa	Number of copies (SEM)	Morphological feature
FliF	61	27.2 (4.4)	M ring
FlgH	22	28.3 (5.0)	L ring
FlgI	36	24.1 (4.3)	P ring
FlgB	15	7.2 (1.2)	Proximal rod
FlgC	14	6.4 (1.1)	Proximal rod
FlgF	26	6.3 (1.4)	Proximal rod
FlgG	28	25.8 (4.3)	Distal rod
FliE	11	9	Unknown

Adapted from Jones *et al.* (5).

Table 2. Comparison of masses (kDa) deduced from subunit stoichiometries (5) with STEM masses of corresponding morphological features

	SUM* (SEM)	Mass† (SEM)
LPRSM (FlgH, -I, -G, -B, -C, -F; FliE, -F)	4300 (352)	4400 (67)
LPR (proximal + distal) (FlgH, -I, -G, -B, -C, -F)	2500 (230)	2600 (51)
LP + distal rod (FlgH, -I, -G)	2200 (225)	2100 (64)
LP (FlgH, -I)	1500 (190)	1700 (11)

*SUM, subunit mass × no. of subunits.
†Mass determined by STEM.

or 12 studs thought to be the MotA–MotB complex (8). The stoichiometry and location of flagellar switch complex (FliG, FliM, and FliN; see ref. 22), which make up another part of the motor, are still unknown.

We thank Charles DeRosier for his skillful assistance in processing the mass data and Beth Y. Lin for help with sample preparations for the STEM. This work was supported by National Institutes of Health Grant GM35433 to D.J.D. and National Institutes of Health Grant RR01777 and a U.S. Department of Energy–Office of Health and Environmental Research grant to the STEM Facility, Brookhaven National Laboratory. Funds to purchase and maintain the computer system were obtained from Shared Instrumentation Grant 1-S10-RR04671-01 awarded to D.J.D. by the National Institutes of Health.

1. Homma, M., Aizawa, S.-I., Dean, G. E. & Macnab, R. M. (1987) *Proc. Natl. Acad. Sci. USA* **84,** 7483–7487.
2. Jones, C. J., Homma, M. & Macnab, R. M. (1987) *J. Bacteriol.* **169,** 1489–1492.
3. Müeller, V., Jones, C., Aizawa, S.-I. & Macnab, R. M. (1992) *J. Bacteriol.* **174,** 2298–2304.
4. Sosinsky, G. E., Francis, N. R., Stallmeyer, M. J. B. & DeRosier, D. J. (1992) *J. Mol. Biol.* **223,** 171–184.
5. Jones, C. J., Macnab, R. M., Okino, H. & Aizawa, S.-I. (1990) *J. Mol. Biol.* **212,** 377–387.
6. DePamphilis, M. L. & Adler, J. (1971) *J. Bacteriol.* **105,** 384–395.
7. Stallmeyer, M. J. B., Aizawa, S.-I., Macnab, R. M. & DeRosier, D. J. (1989) *J. Mol. Biol.* **205,** 519–528.
8. Khan, S., Dapice, M. & Reese, T. S. (1988) *J. Mol. Biol.* **202,** 575–584.
9. Wall, J. S. & Hainfeld, J. (1986) *Annu. Rev. Biophys. Biophys. Chem.* **15,** 355–376.
10. Engel, A. (1978) *Ultramicroscopy* **3,** 273–281.
11. Jones, C. J., Homma, M. & Macnab, R. M. (1989) *J. Bacteriol.* **171,** 3890–3900.
12. Homma, M., Kutsukake, K., Hasebe, M., Iino, T. & Macnab, R. M. (1990) *J. Mol. Biol.* **211,** 465–478.
13. Homma, M., DeRosier, D. J. & Macnab, R. M. (1990) *J. Mol. Biol.* **213,** 819–832.
14. Aizawa, S.-I., Dean, G. E., Jones, C. J., Macnab, R. M. & Yamaguchi, S. (1985) *J. Bacteriol.* **161,** 836–849.
15. Wall, J. S. (1979) in *Introduction to Analytical Electron Microscopy*, eds. Hsen, J. J., Goldstein, J. I. & Joy, D. (Plenum, New York), pp. 333–342.
16. Wall, J. S., Hainfeld, J. F. & Chung, K. D. (1985) *Proc. Annu. Meet. Electron Microsc. Soc. Am.* **43,** 716–717.
17. Engel, A., Christen, F. & Michel, B. (1991) *Ultramicroscopy* **7,** 45–54.
18. Wagenknecht, T., DeRosier, D. J., Aizawa, S.-I. & Macnab, R. M. (1982) *J. Mol. Biol.* **162,** 69–87.
19. Snedecor, G. W. & Cochran, W. G. (1967) *Statistical Methods* (Iowa State Univ. Press, Ames).
20. Akiba, T., Yoshimura, H. & Namba, K. (1991) *Science* **252,** 1544–1545.
21. Blair, D. F. & Berg, H. C. (1988) *Science* **242,** 1678–1681.
22. Yamaguchi, S., Aizawa, S.-I., Kihara, M., Isomura, M., Jones, C. J. & Macnab, R. M. (1986) *J. Bacteriol.* **168,** 1172–1179.